*Review* _____ *Forma*, **17**, 211–238, 2002

# Reconnection of Line Singularities—Description and Mechanism

Ryuji TAKAKI

*Tokyo University of Agriculture and Technology, Koganei, Tokyo 184-8588, Japan*
*E-mail address: takaki@cc.tuat.ac.jp*

(Received August 19, 2002; Accepted October 31, 2002)

**Keywords:** Reconnection, Vortex Filaments, Dissipative Effect, Topology Change, Line Singularities

**Abstract.** Reconnection process of line singularities in the viscous fluid is explained and possible interpretations on its mechanism are given. Reconnection processes in various other physical systems are also explained, such as the vortex filaments in the superfluid, the disclinations in liquid crystals and the magnetic lines in plasmas. Similarities among these processes are suggested. It is emphasized that dissipative effects within the narrow region where the reconnection is taking place is essential for its occurrence.

## 1. Introduction

There are several kinds of line singularities appearing in continuum materials. The term “singularity” indicates a state where a certain physical quantity in materials, such as density, velocity or stress, has different values along a straight or curved line from those out of this line. In many cases they play important roles for global behavior of the materials in spite of the fact that the volume fractions of the line singularities are quite small, because the singularities often possesses large energies so as to govern the dynamics of the whole materials.

The most popular example of such line singularities would be the vortex filament appearing in fluids with low viscosity. The real fluids familiar to us have finite viscosities. But, the vortex with filament shape can appear if the viscosity is small enough or the fluid velocity is large enough. Only one exception in the real fluids is the superfluid helium, which has completely zero viscosity. The case of the superfluid is discussed later along with line singularities in other systems.

A familiar vortex filament appearing in the nature is the tornado (see Fig. 1(a)). We can observe a tornado easily since it is made of a dark or an opaque column. This column is visible because of the dust or the water droplets suspended within it. However, the dynamical nature of the tornado is not the suspended elements but the velocity distribution of the air within and around it. As is shown in Fig. 1(b), the air within a tornado is rotating around the central axis just like a solid cylindrical body, i.e. the velocity of the air is proportional to the distance from the axis. On the other hand, the air out of the tornado is

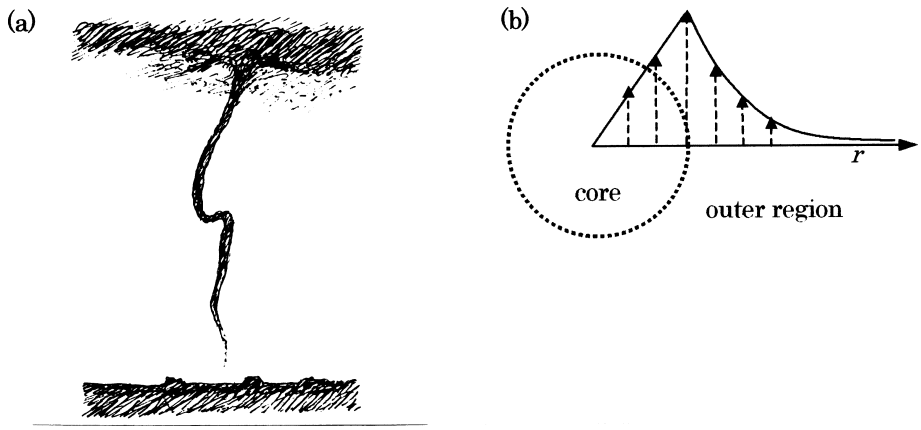


Fig. 1. (a) Sketch of a tornado and (b) the velocity distribution within and out of a tornado.

moving around the tornado with the velocity which is inversely proportional to the distance from the axis. Therefore, the velocity takes its maximum value on the surface of the tornado. Note that this velocity distribution is common among many vortical structures in open space, including typhoon and ocean eddy.

Vortex filaments show various kinds of motions. When a filament is deformed from a straight shape, it continues to deform further owing to the velocity induced by the filament itself (ARMS and HAMA, 1965; BETCHOV, 1965; HASIMOTO, 1971; TAKAKI, 1975). When two filaments with the same sense of rotation get near to each other, they are apt to tangle with each other to form a double helix (CHANDRSUDA *et al*., 1978; HOPHINGER *et al*., 1982; TAKAKI and HUSSAIN, 1984a, b). These motions can be understood in terms of the dynamics without effect of viscosity (BATCHELOR, 1967), hence its analysis is relatively simple. A general introduction to vortex dynamics, especially the deformation and entanglements are given by TAKAKI (1988).

The third type of motion is a quick topological change played by two vortex filaments with the opposite sense of rotation, when they get near to each other. This motion is called "reconnection" or "recombination". Examples of observations of this motion are shown in Fig. 2. Figure 2(a) shows two trailing vortices from an aircraft, which approached each other and made successive reconnections to form a street of ring vortices (CROW, 1970). Figure 2(b) shows an observation in laboratory (HAMA, 1960), where a part of a line vortex was separated to form a ring vortex through reconnection. Figure 2(c) shows a laboratory experiment to observe behavior of two vortex rings, which made a reconnection to form a large ring (OSHIMA and ASAKA, 1977). As is seen from these figures, when parts of vortices get near, each of those parts is cut suddenly and reconnected to the other. This topological change of filaments occurs much more rapidly than those of other parts of filaments.

In the next section the basic characteristics of vortex filament are explained. A review of past researches of the reconnection process is given in Sec. 3, including the cases in other materials, where similarities of these processes with that in the viscous fluid is discussed.

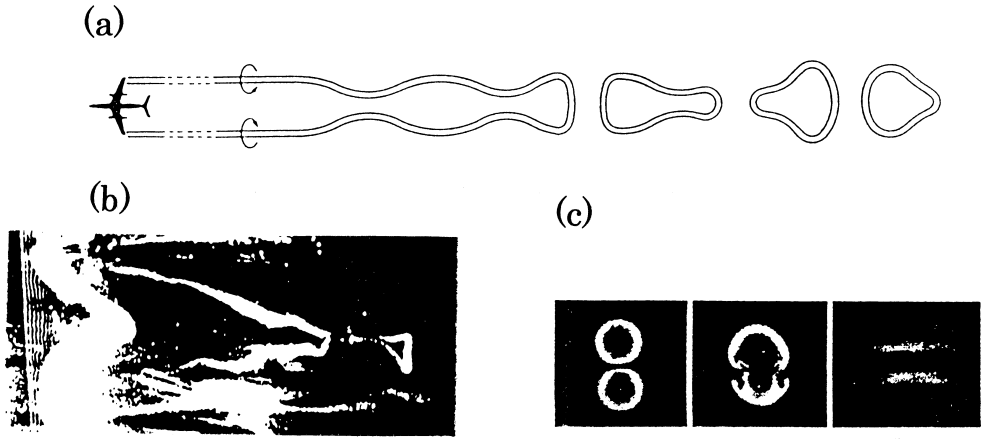


Fig. 2. Observed reconnection processes. (a) Sketch of formation of vortex rings from a photograph by CROW (1970), (b) separation of a ring shape vortex from a line vortex from HAMA (1960), (c) merging of two vortex rings from OSHIMA and ASAKA (1977)

In Sec. 4 some results of experiment and computation by the present author are presented. In the last section essential natures of this phenomenon are noted. This paper includes some experimental data obtained from the present author but not published yet. However, this paper is written as a review article, since most of its contents are already known.

## 2. Basic Characteristics of Vortex Filament

### *2.1. Definition of vortex filament*

For definition of the vortex filament it is necessary to define the vorticity vector in a three-dimensional space. Let the velocity vector in a fluid be denoted by

$$\boldsymbol{u}(x,y,z,t) = \big(u(x,y,z,t), v(x,y,z,t), w(x,y,z,t)\big). \tag{1}$$

Then, the vorticity vector $\omega(x, y, z, t)$ is defined by a differential operation of the velocity vector as follows:

$$\omega(x, y, z, t) = \text{rot } \boldsymbol{u}(x, y, z, t). \tag{3}$$

In general, the differential operator "rot" gives the strength of rotation of vector field, and the vorticity stands for the strength of rotation of a fluid element around its center. Note that a fluid element does not have a vorticity if it does not rotate around its center, even when it is moving along a circular orbit. The direction of the vorticity vector is parallel to the rotation axis and coincides with the direction of the right-screw.

Now, the vortex filament is a distribution of vorticity confined in a thin filament-like

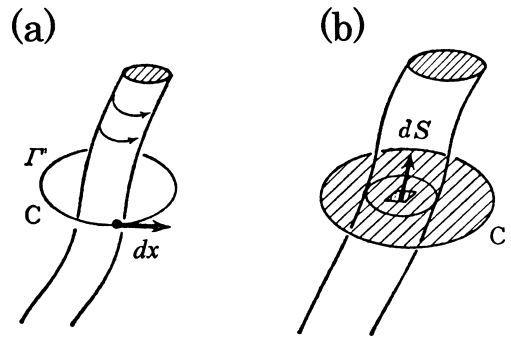


Fig. 3. Definition of the circulation. (a) Path integral along the curve C surrounding the filament, (b) surface integral in a region intersecting with the filament.

region, as is shown by the rough sketch in Fig. 1. This region is called a "core" of the filament. It can be proved easily, by the use of a formula of the vector analysis, that the vortex filament does not terminate within the fluid, i.e. it should either terminate at a solid (or free) boundary or form a loop by itself. In fact the lower end of a tornado is attached to the earth (or sea) surface. Its upper end is expanding horizontally and should finally reach the earth at far places.

The vortex with a ring shape is called a "vortex ring" or a "ring vortex". A vortex ring can be easily produced by ejection of a small amount of fluid through a circular orifice. If an elliptic orifice or other types of orifices are used, vortex rings with various shapes are produced.

Strength of a vortex filament is expressed in terms of a quantity $\Gamma$ called a "circulation", which is defined by a path integral of velocity vector or a surface integral of the vorticity, as follows:

$$\Gamma = \oint \boldsymbol{u} \cdot d\boldsymbol{x} = \iint \omega \cdot d\boldsymbol{S}. \tag{3}$$

where the path integral is taken along a closed curve surrounding the filament and the surface integral is taken over a region within this closed curve (see Fig. 3).

If the path is chosen to a circle with the center at the core and the radius $r$, then the above path integral gives $\Gamma = 2\pi r u$. It can be proved that $\Gamma$ does not depend on the choice of the closed curve if it is located out of the core. This fact shows that $\Gamma$ is a quantity characteristic of a vortex filament and that the velocity is inversely proportional to $r$ in the region out of the core, i.e. $u = \Gamma/2\pi r$.

*2.2. Vortex filament in the viscous fluid*

The velocity distribution within the core can not be determined uniquely from the above definition of vorticity or circulation. It depends on properties of the fluid. In the case of the viscous fluid the vorticity is nearly proportional to the radius $r$, as shown in Fig. 1(b). Then, the vorticity is uniform within the core (proved by the use of Eq. (2)), and the

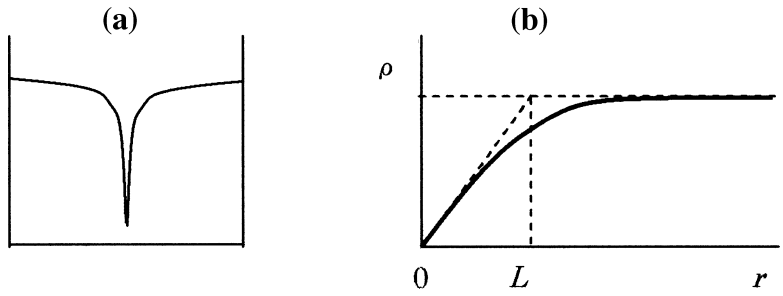


Fig. 4. (a) Side view of a vortex filament in superfluid helium formed in a container, where the core is a hollow space owing to the strong effect of centrifugal force, (b) a solution of the Gross-Pitaevskii equation for a vortex filament. The density $\rho$ is defined by the square of absolute value of the wave function. The core size $L$ has a scale of the inter-molecular distance.

circulation is simply a product of the vorticity $\omega$ and the cross section $S$ of the core, i.e. $\Gamma = \omega S$.

The radius $R$ of the filament cross section is in many cases grows with time slowly according to the formula:

$$R = \sqrt{\nu t} \tag{4}$$

where $\nu$ is the kinematic viscosity defined by $\nu = \mu/\rho$ ($\mu$ is the viscosity and $\rho$ is the density). Hence, the core cross section grows owing to a dissipative effect.

Since the vortex core is governed by the viscosity, we can guess easily that the reconnection process is also affected much by the viscous effect. This possibility is confirmed in the next section.

*2.3. Vortex filament in the superfluid helium*

Vortex filament can appear in the superfluid helium, i.e. the liquid helium below the $\lambda$ point (2.18 K). As for the flow field out of the filament there is no essential difference between the viscous fluid and the superfluid. The peculiarity of the superfluid is that the circulation is quantized as

$$\Gamma = \frac{h}{m} = 1.0 \times 10^{-3} \left(\mathrm{cm}^2 / \mathrm{s}\right) \tag{5}$$

where $h$ is the Planck's constant and $m$ is the mass of helium atom. The flow field near the vortex filament is obtained theoretically by GROSS (1961) and PITAEVSKII (1961) by the use of the hydrodynamic representation of the Schrödinger equation (called Gross-Pitaevskii equation). According to their theory the velocity is proportional to $1/r$ down to the core center, while the density vanishes at the core center. The core has a magnitude of the molecular size. The singularity of the velocity field at the center does not lead to a

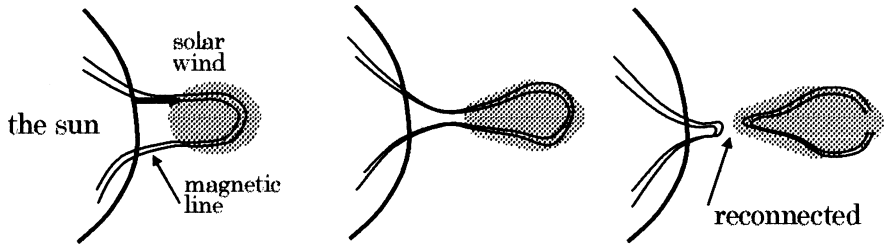


Fig. 5. Extraction of the solar magnetic lines and their reconnection.

difficulty, because molecules do not exist at the center (0 density).

Vortex filament in the superfluid has been observed through the following experimental procedure. Put the liquid helium above the $\lambda$ point (normal fluid) in a small container and rotate the container. The liquid helium begins to rotate like a solid body rotation (uniform vorticity) owing to its viscosity. Lower the temperature below the $\lambda$ point while rotating the container. Then, the flow field in the liquid stops suddenly to have a vorticity and discrete vortex filaments are produced. Through this process the vorticity is not lost but has changed its distribution from a continuous to discrete one. Mechanism of this change is not understood yet! It is a rapid transition from a classical state to a quantum state of a system with macroscopic scale.

*2.4. Magnetic lines in plasma*

It is well known that each of the magnetic lines has a tension along itself, while they produce repulsive forces among themselves. Therefore, magnetic field tends to expand laterally according to this repulsion. However, if the magnetic lines are formed within a plasma with high electric conductivity, the magnetic lines may keep a form of thin bundle, because the magnetic lines are frozen to the plasma and because the plasma will act to hold the magnetic lines (this situation is called "frozen"). Such a configuration of magnetic lines and plasma is seen in the solar wind.

When the solar wind is ejected from the sun, the wind extracts magnetic lines from the solar surface and expands them. But, since the magnetic lines have a tension, they can not be expanded infinitely. Actually, nearby magnetic lines with opposite directions make a reconnection process and a separated loops of magnetic lines are produced, which are allowed to travel far from the sun.

Here it is noted that there is a close similarity between the fluid motion and the magnetic field in a plasma. If the electric current density in the plasma and the magnetic field are denoted by $\boldsymbol{i}$ and $\boldsymbol{H}$, respectively, they are related by a formula (one of the Maxwell's equations),

$$\boldsymbol{i} = \mathrm{rot}\boldsymbol{H}, \tag{6}$$

which is similar to Eq. (2). Similarities of the vorticity field and the magnetic field are discussed in Subsec. 3.3.

## 3. Mechanism of Reconnection

### *3.1. Review of studies of reconnection process in the viscous fluid*

Past researches of the reconnection process in the viscous fluid are mostly experimental and computational ones, and few works have been made theoretically except that by YEH and AXFORD (1970) for plasma and that by the present author (TAKAKI and HUSSAIN, 1985, 1988). Because the reconnection process is a really complicated problem and theoretical formulation is quite difficult. In fact the fluid motion in this process is (i) three-dimensional, (ii) transient, (iii) nonlinear and (iv) dissipative. If any of these factors is missing, the essential feature of the process is lost. Therefore, analysis of the reconnection process still continues to be a big challenge for theoretical physicists. Some important contributions are introduced below. A precise survey on this phenomenon is written by KIDA and TAKAOKA (1994).

The first report on this phenomenon was made by HAMA (1960), in which a vortex filament produced in a boundary layer along a flat plate deformed and its small part was cut apart from the filament (see Fig. 2(b)). However, since this phenomenon was not the main purpose of his study, it was not described precisely. Next, a street of ring-type vortices was observed in a pair of trailing vortices behind an aircraft (CROW, 1970). The photograph of reconnection in this paper was taken by chance (see Fig. 2(a)). The present author also had a chance to see the same phenomenon, but failed in taking photograph. Experiments aimed at observing the reconnection were made by KAMBE and TAKAO (1971), FOHL and TURNER (1975) and OSHIMA and ASAKA (1977). In the experiment of KAMBE and TAKAO (1971) a single elliptic ring vortex was ejected and production of two or more vortices was observed, where two parts of the initial vortex approached and made a reconnection. In most of other experiments, two vortex rings were ejected nearby in the same direction. Then, they made a reconnection to form a single vortex (see Fig. 2(c)), followed by the second reconnection process producing two vortex rings again. In these experiments global behavior of vortex rings were observed by the use of a visualization technique.

Numerical computations of the reconnection process were made by several researchers (MELANDER and ZABUSKY, 1988; KIDA and TAKAOKA, 1988; ASKMAN and NOBIKOV, 1988; MELANDER and HUSSAIN, 1989). These numerical results agreed well with experiments, hence it is certain that the vorticity field is actually making a rapid change to form a new field with reconnected state. Although there is a finding that some fraction of vorticity in the original vortex filaments remains connected as in the initial state (MELANDER and HUSSAIN, 1989; KIDA *et al*., 1991), the main part of filaments are reconnected. At present there seems to be no active research of the reconnection process, because, probably, new findings are not much expected compared to the amount of efforts for it.

### *3.2. A proposed mechanism of the reconnection mechanism*

The theory by TAKAKI and HUSSAIN (1985, 1986, 1988) treats the flow field in a local region, where the reconnection process is taking place. This region includes the vortex cores and has a size smaller than the core radius (hatched region in Fig. 6(a)). In such a narrow region the flow field is looked upon as laminar (not turbulent) and the velocity distribution can be expressed by relatively simple functions of coordinates.

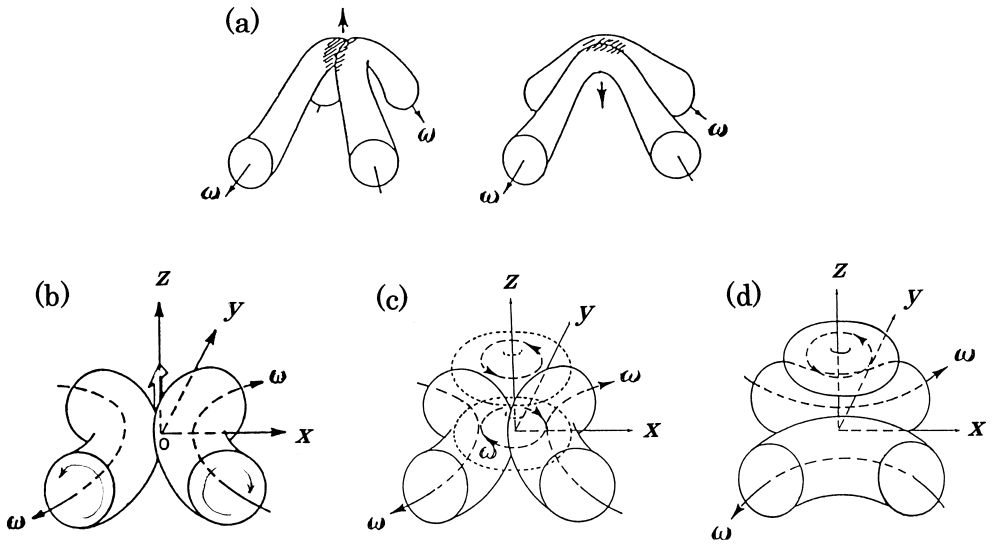


Fig. 6. (a) A rough sketch of the reconnection process, (b) the initial state, (c) superposition of vortex rings on the initial state, (d) the final state.

The flow behavior in the initial and final states can be estimated by considering the spatial symmetries of velocity field and the orders of magnitude of velocity components. Let the initial and the final states include vortex filaments directed nearly to the *y*-axis and *x*-axis, respectively, as shown in Figs. 6(b) and (d). The velocity at the center (the origin) is directed in the positive *z*-direction (shown by a thick arrow in Fig. 6(b)). In these states the *x*-, *y*- and *z*-components of the velocity vector ($u$, $v$, $w$) can be assumed to have symmetries as shown in Table 1. Note that the both states have the same symmetries, and that the symmetry with respect to *z* can not be assumed since the filaments are deformed into curved lines, which are convex to the positive *z*-direction owing to the upward velocity (see Fig. 6(a)).

Next, in the initial state the fluid is moving along circular paths on vertical planes which is nearly parallel to the *xz*-plane, hence $v$ should have small values everywhere around the origin while $u$ and $w$ have no such constraints. Moreover, velocity components do not depend much on *y*. In the final state, where the fluid is moving almost in the *yz*-plane, $u$ has a small value and velocity components do not depend on *x*. The component $w$ continues to have a large value throughout the reconnection process. From these considerations we can obtain terms of polynomial expansions of components as listed in Table 1 (for precise see Appendix A).

The vorticity fields in the initial and final states are obtained by the use of Eq. (2) and the fact that the vorticity is directed initially in the *y*-direction and finally in the *x* direction. Symmetries of vorticity components and possible polynomial terms are given in Appendix A.

Table 1. Symmetries of velocity components with respect to coordinates.

| | Initial state | | | | | | Final state | | | | | |
|---|---|---|---|---|---|---|---|---|---|---|---|---|
| | $x$ | $y$ | $z$ | 0th | 1st | 2nd | $x$ | $y$ | $z$ | 0th | 1st | 2nd |
| $u$ | odd | even | — | — | $x$ | $xz$ | odd | even | — | — | — | — |
| $v$ | even | odd | — | — | — | — | even | odd | — | — | $y$ | $yz$ |
| $w$ | even | even | — | 1 | $z$ | $x^2, z^2$ | even | even | — | 1 | $z$ | $y^2, z^2$ |

The symbol "—" means no symmetry, and "0th", "1st", "2nd" mean possible polynomials up to the second order of coordinates (a more precise table is given in Appendix A).

Next, it is necessary to give a mechanism for transition from the initial to the final state. If we observe this process from the $z$-direction, parts of the vortex filaments going through the $xz$-plane should disappear, and new filaments through the $yz$-plane should appear to connect the four ends of the filaments. This process can be realized by superposing a pair of vortex rings on the two filaments as shown in Fig. 6(b), where the lower vortex ring cancels the parts of filaments going through the $xz$-plane and at the same time makes new bridges through the $yz$-plane. Another vortex ring is necessary for momentum conservation of the fluid. These vortex rings grow with time, so that its superposition on the initial state leads to the final state. Moreover, the ring has an axisymmetry around the $z$-axis and the magnitude of the velocity is expressed by a polynomial function of $z$ and $r^2 = x^2 + y^2$. Polynomial expansion of this ring field $\boldsymbol{u}^{(r)}$ is also necessary (given in Appendix A).

After all, we can express the reconnection process by the following equation for the velocity fields:

$$\boldsymbol{u}^{(i)} + \boldsymbol{u}^{(r)}(t) \to \boldsymbol{u}^{(f)}. \tag{7}$$

Here, we make another assumption that the fluid velocity expressed by $\boldsymbol{u}^{(r)}$ proceeds with time $t$ everywhere with the same pace, i.e. the coefficients in the polynomial expansions of $\boldsymbol{u}^{(r)}$ depend on $t$ through a single function $T(t)$. Then, the problem is reduced to obtaining this function by the use of the governing equation for flow field.

The polynomial expansions should be made also for the vorticity components. After considering their symmetries and orders of magnitude, we can obtain the following polynomial expansions (for precise see Appendix A):

$$u = -m(1 - T(t))x + k(1 - T(t))xz, \tag{8a}$$

$$v = mT(t)y + kT(t)yz, \tag{8b}$$

$$w = w_0 - \delta T(t) + m(1 - 2T(t))z - l(1 - T(t))x^2/2 + lT(t)y^2/2 + k(1 - 2T(t))z^2/2, \tag{8c}$$

$$\omega_x = (k + l)T(t)y - nT(t)yz, \tag{9a}$$

$$\omega_y = (k + l)(1 - T(t))x - n(1 - T(t))xz, \tag{9b}$$

$$\Delta\omega_x = g_x T(t)y, \tag{10a}$$

$$\Delta\omega_y = g_y(1 - T(t))x, \tag{10b}$$

where Laplacians of the vorticity components in Eqs. (10a) and (10b) are necessary in applying the governing equation. The function $T(t)$ should begin with value 0 and asymptote to 1 for $t \to \infty$.

Equation for $T(t)$ can be derived from the vorticity equation (which is derived from the Navire-Stokes equation),

$$\partial\omega/\partial t + (\boldsymbol{u}\nabla)\omega - (\omega\nabla)\,\boldsymbol{u} = \nu\Delta\omega, \tag{11}$$

where $\nu$ is the kinematic viscosity. The second and the third terms of the left-hand side of Eq. (11) stand for the convection of vorticity by fluid motion and the thinning of vorticity distribution by stretching, respectively. The right-hand side stands for the viscous diffusion of vorticity. Substituting the above expansions into this equation, we obtain after some manipulation the following equation:

$$\mathrm{d}T/\mathrm{d}t - t^{*-1}T + t^{*-1}T^2 = 0, \tag{12}$$

where $t^*$ is a constant with dimension of time defined as follows:

$$t^* = \delta n/(k + \mathrm{l}) = \nu(g_x - g_y) - 2m. \tag{13}$$

The solution of Eq. (12), satisfying the boundary conditions $T(-\infty) = 0$, $T(\infty) = 1$, is

$$T(t) = e^{t/t^*} \Big/ \left(1 + e^{t/t^*}\right). \tag{14}$$

Behavior of $T(t)$ is shown in Fig. 7. As is seen from this figure, the flow field makes a transition within a time scale of $t^*$. In order that $t^*$ be positive, we must have $g_x > g_y$, i.e. the Laplacian of the initial vorticity should be larger than that of the final vorticity. It would mean that the initial vortex filament was thinner than the final one, and that the vorticity has defused through the reconnection process.

The values of coefficients $k$, $l$, $m$, $n$ and $\delta$ remains undetermined except that they have positive values, as will be seen by careful observation of vortex configuration in Fig. 6. They could, however, be determined in principle, if the flow field out of the local region around the origin is given. Therefore, the main result in this anlysis is that the local flow behavior concerning to the reconnection process can be determined to a certain degree without knowledge of the outer field. This fact seems to suggest that the local motion in the reconnection process has a common behavior among situations with different outer flow fields.

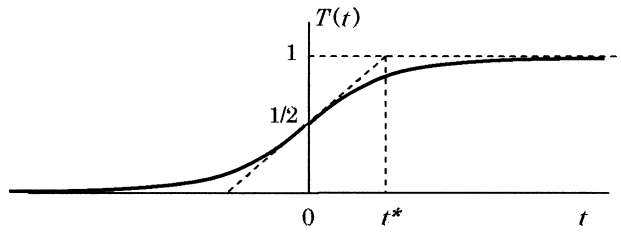


Fig. 7. Solution of $T(t)$. $t^*$ is a time scale of reconnection process.

By choosing these coefficients appropriately, we can draw vorticity lines (group of the curve on which the vorticity vector is tangent to it) at each instant of reconnection process, as shown in Fig. 8. Note that this figure is not showing vortex filaments, but vorticity lines starting from several points arranged on two circles. However, it depicts well how the vorticity behaves at the center of reconnection.

The role of viscosity in the reconnection process can be examined in general way by applying the vorticity equation (11) to the flow field on the *yz*-plane. If the reconnection takes place and the final state (Fig. 6(d)) appears, the *x* component of the vorticity should grow on the *yz*-plane. It can be shown that this component can appear only in the presence of viscosity (see Appendix B). This fact will suggest a general necessary condition for reconnection processes in various physical systems, i.e. a certain dissipative effect should play an important role at the region of reconnection. In the following sections, mechanisms of reconnection are explained based on this idea.

### *3.3. Similarity of mechanisms between the viscous fluid and the plasma*

The reconnection process of magnetic field in plasma in the 2D space is solved theoretically by YEH and AXFORD (1970). In this analysis two fields, the inner field around the center of reconnection and the outer field far from the origin, are treated separately and then matched to each other. As is shown in Fig. 9, the magnetic lines are convected by plasma flow (since the magnetic field is frozen in the plasma) in the *x*-direction, reconnected in the inner region and convected away to both sides of *y*-direction. This solution is stationary and has no dependence on time. Time-dependent and 3D solutions are obtained later (Terasawa *et al*., private communication, 1992), but the solution by YEH and AXFORD (1970) is enough for the present purpose to compare the cases of viscous fluid and magnetic field.

It is noted here that there are two ways of analogy between the vorticity field and the magnetic field. One is based on the similarity of Eqs. (2) and (6), where the velocity $\boldsymbol{u}$ corresponds to the magnetic field $\boldsymbol{H}$, and the vorticity $\omega$ to the current density $i$. In this analogy, the reconnetion of vortex filaments does not directly correspond to that of magnetic lines. Another analogy is based on the governing equations of both fields, where the vorticity is governed by Eq. (11) and the magnetic field in plasma by the following equation:

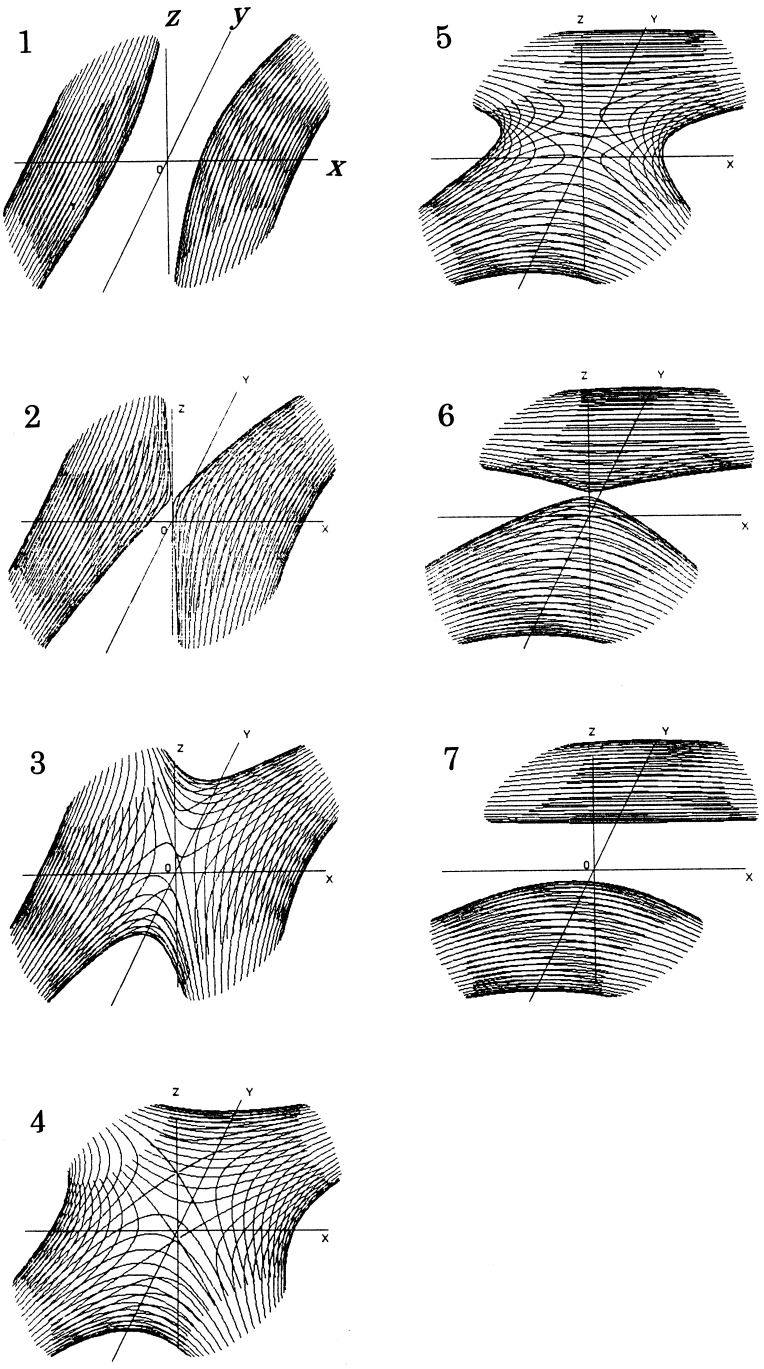


Fig. 8. Theoretical results for changes of vorticity lines in reconnection process (from TAKAKI and KAKIZAKI, 1992).

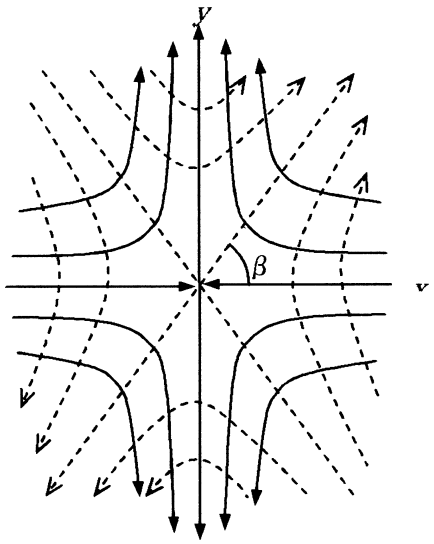


Fig. 9. 2D motions of magnetic lines (dashed lines) convected by the plasma flow (solid lines). Magnetic lines are reconnected at the origin. Sketch from the figure in the paper of YEH and AXFORD (1970).

$$\partial \boldsymbol{H}/\partial t + (\boldsymbol{u}\nabla)\boldsymbol{H} - (\boldsymbol{H}\nabla)\,\boldsymbol{u} = \eta\Delta\boldsymbol{H}, \tag{15}$$

where $\eta$ is defined by $\eta = 1/(\sigma\mu_0)$, $\sigma$ is the electric conductivity of the plasma and $\mu_0$ is the magnetic permeability. This equation is derived by combining the Maxwell's equation and the fluid dynamical equation along with Ohm's law. As in the vorticity field, the second and the third terms of the left-hand side of Eq. (15) stand for the convection of magnetic lines by fluid motion and the thinning of bundle of magnetic lines by stretching, respectively. The right-hand side stands for the diffusion of magnetic lines by electric conductivity. By comparing Eqs. (11) and (15), we can convince ourselves that the magnetic lines correspond to vortex filaments so long as their dynamics are concerned.

After examination of the solution of YEH and AXFORD (1970), it can be shown that their inner solution is similar to that obtained by the present author at the time with $T(t) = 1/2$, i.e. at the intermediate time of reconnection, and at $z = 0$, if unknown coefficients are chosen appropriately (TAKAKI, unpublished). Comparison of both solutions are shown in Table 2.

As seen in this table, both fields correspond to each other quite well, if $1/(\cos 2\beta) >> 1$, i.e. $\beta \fallingdotseq \pi/4$. It is an interesting fact that the vector field $A$ corresponds to the upward velocity $w$ in the viscous fluid. It has come from the relation of the vector potential vector $(0, 0, A)$ and the magnetic flux $B$ through $B = \mathrm{rot}A$, which is analogous to Eq. (2).

It should be stressed that the reconnection of magnetic lines is possible only when the plasma has a finite electric conductivity, i.e. a dissipative effect. This situation corresponds to the fact that the vortex reconnection requires finite a viscosity, i.e. also a dissipative effect.

Table 2. Comparison of the solutions of magnetic field (YEH and AXFORD, 1970) and vorticity field (TAKAKI and HUSSAIN, 1988).

| Magnetic field | Vorticity field at $z = 0$, $T(t) = 1/2$ |
|---|---|
| Finite conductivity important | Viscosity important |
| 2D flow | 3D flow |
| Stationary | Time dependent via $T(t)$ |
| Inner and outer fields matched | Inner field only |
| $u = -2\gamma x$, $v = 2\gamma y$ | $u = -mx/2$, $v = my/2$ |
| $A = -\sigma\mu_0 E\{(x^2 + y^2) - (x^2 - y^2)/\cos 2\beta\}/4$ | $w = -l(x^2 - y^2)/2$ |
| $B_x = -\sigma\mu_0 E\{1 + 1/(\cos 2\beta)\}y/2$ | $\omega_x = ly/2$ |
| $B_y = \sigma\mu_0 E\{1 - 1/(\cos 2\beta)\}x/2$ | $\omega_y = ly/2$ |

$A$, $B_x$, $B_y$ are the vector potential and components of magnetic flux, respectively.

### *3.4. Reconnection of vortex filaments in superfluid*

Reconnection of quantized vortex filaments in the superfluid helium has been attracting interests of scientists. It was once considered to be a main mechanism for production of a kind of excitation called "roton" in superfluid (FEYNMANN, 1955), but this conjecture is not supported now. At present, the reconnection is considered to be responsible for quantum turbulence (turbulent motions of a lot of quantized vortices) in the superfluid (TOUGH, 1982; DONNELLY, 1991). Behavior of quantized vortices are simulated numerically by (SCHWARZ, 1985, 1988; TSUBOTA and MAEKAWA, 1992). However, there seems to be still no theory to describe how vorticies can reconnect themselves.

Here, it is suggested that an introduction of a certain dissipative effect into dynamics of superfluid may allow occurrence of reconnection (TAKAKI, unpublished). For its explanation we need a hydrodynamic representation of the Schrödinger equation for helium atoms (GROSS, 1961; PITAEVSKII, 1961). Let one-body wave function of helium atom and the interaction potential between them be denoted by $\Psi$ and $V_0\delta(\boldsymbol{r}_i - \boldsymbol{r}_j)$, respectively, where $\delta$ is the 3D delta function. Then, the Schrödinger equation is written as

$$i\hbar\frac{\partial\Psi}{\partial t} = -\frac{\hbar^2}{2m}\nabla^2\Psi + V_0|\Psi|^2\Psi. \tag{16}$$

Next, from $\Psi$ and its phase $S$, we define the density and the velocity of superfluid as follows:

$$\rho(r) = m|\Psi|^2, \quad \boldsymbol{u}(r) = (\hbar/m)\nabla S. \tag{17}$$

Substituting Eq. (17) into Eq. (16) we obtain after some manipulations the following equations for $\rho$ and $\boldsymbol{u}$:

$$\dot{\rho} + \nabla(\rho \boldsymbol{u}) = 0,$$
$$\dot{\boldsymbol{u}} + (\boldsymbol{u}\nabla)\boldsymbol{u} = -\nabla\left\{\frac{V_0}{m^2}\rho - \frac{\hbar^2}{2m^2}\frac{\nabla^2\sqrt{\rho}}{\sqrt{\rho}}\right\} \equiv -\nabla P, \tag{18}$$

where the first equation has the same form as the continuity equation for the ordinary fluid and the second is essentially the Euler's equation (an equation for inviscid fluid) with pressure $P$. Therefore, the motion of superfluid governed by Eq. (18) has no dissipative effect, and the reconnection will not be described with this equation.

Behavior of superfluid with a finite temperature (below the $\lambda$ point) is often described by the so-called two-fluid model, where the fluid is looked upon a mixture of a super part with density $\rho_s$ and a normal part with density $\rho_n$. The both parts can have different flow velocities, say $\boldsymbol{u}_s$ and $\boldsymbol{u}_n$. Since the superfluid is composed of a single material, helium atoms, this decomposition into both parts is merely a phenomenological model. However, it is a convenient model for describing various phenomena, such as the second sound (a wave transmitting the entropy). It is sometimes assumed that both parts receive a mutual friction, so that the force on the unit volume of the super part is written as follows:

$$\boldsymbol{f} = \rho_s\rho_n\{A(\boldsymbol{u}_n - \boldsymbol{u}_s) + B|\boldsymbol{u}_n - \boldsymbol{u}_s|^2(\boldsymbol{u}_n - \boldsymbol{u}_s)\}, \tag{19}$$

where $A$ and $B$ are positive constants.

Since Eq. (18) is looked upon as a governing equation for the super part, $\boldsymbol{u}$ in Eq. (18) is replaced with $\boldsymbol{u}_s$. Here, an assumption is made as to the behavior of the normal part in a region near to vortex filaments. Since $\boldsymbol{u}_n$ is much weaker than $\boldsymbol{u}_s$, which is inversely proportional to the distance from the core center (this distance is comparable to the intermolecular distance), the velocity of the normal part, which is always suppressed by the viscosity, can be negligible, hence we can assume $\boldsymbol{u}_n = 0$ and $\rho_n = $ const. in the region of reconnection.

Now, by adding the above frictional force to the right-hand side of Eq. (18) and making a differential operation "rot" on both sides of it, we have the following equation for the vorticity $\omega = \mathrm{rot}\boldsymbol{u}_s$:

$$\partial\omega/\partial t + (\boldsymbol{u}_s\nabla)\omega - (\omega\nabla)\boldsymbol{u}_s$$
$$= -\rho_s\rho_n\{A + B|\boldsymbol{u}_s|^2\}\omega - A\nabla(\rho_s\rho_n) \times \boldsymbol{u}_s - B\nabla(\rho_s\rho_n\,|\boldsymbol{u}_s|^2) \times \boldsymbol{u}_s. \tag{20}$$

We try to speculate on the effects of these terms in the region between two oppositely directed vortex filaments, as shown in Fig. 10. The second and the third terms in the left-hand side of Eq. (20) are convection and stretching terms, which are not important here. The first term in the right-hand side is directed always opposite to the vorticity, hence it is a decay term due to the mutual friction. The second term in the right-hand side is also a decay term, because the gradient $\nabla(\rho_s\rho_n)$ is directed outwards from the core center (see Fig. 4(b)) and its vector product with $\boldsymbol{u}_s$ (circulating around the core) is directed opposite to $\omega$. On the other hand, the third term is effective for reconnection, as is seen from the following consideration. If the filaments are curved convex to the origin (see Fig. 10(a)), the vertical

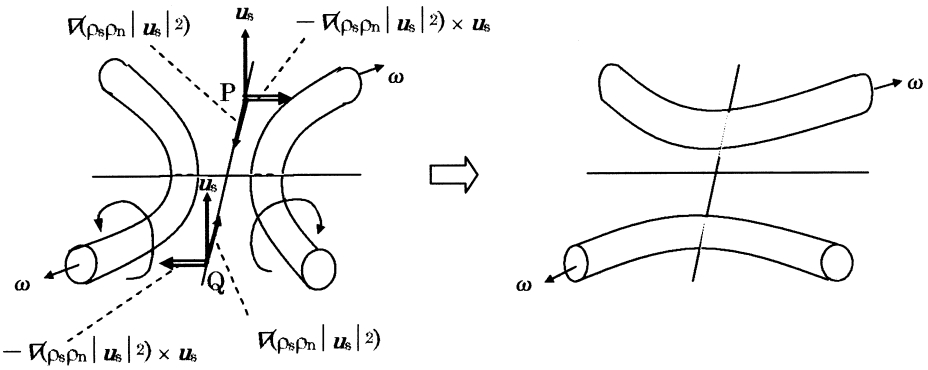


Fig. 10. Growths of a rightward and a leftward vorticities at the points P and Q, respectively, which lead to a reconnected configuration of vortices.

velocity on the *yz*-plane increases towards the origin and the gradient of $(\rho_s\rho_n|\boldsymbol{u}_s|^2)$ is directed to the origin. Then, its vector products with $\boldsymbol{u}_s$ at the points P and Q in Fig. 10(a) produce vorticities directed rightward and leftwards, respectively. Thus, bridges are produced at these points to reconnect the filaments, as shown in Fig. 10(b).

This story of vortex behavior seems promising for explanation of reconnection process in superfluid helium. But, it contains some difficulties. First, the change of vorticity described above contradicts with the general idea of super part, i.e. it is an inviscid fluid and vorticity should not appear owing to the Kelvin's vorticity theorem. Secondly, the change of vorticity contradicts with the concept of quantized circulation given by Eq. (5). Therefore, the above speculation must be replaced by a proper analysis of vortex behavior with quantum jump, where an interaction between the filaments and certain kinds of excitations with vortical nature should play an important role.

### *3.5. Reconnection of disclinations in liquid crystals*

Liquid crystal is a material made of molecules with coherence in their orientations. Distribution of the orientations is expressed in terms of unit vector, called a director. Note that each director is like a line segment and not like an arrow, because the molecule has no distinction with its reversed state. However, the director distribution has a close analogy with the velocity field of inviscid fluid.

In the 2D director distributions, where the directors are parallel to a plane, say *xy*-plane, components of director $(u, v)$ are expressed in terms of a harmonic function $\phi(x, y)$ as follows:

$$u = \cos\phi, \quad v = \sin\phi, \quad \text{where } \Delta\phi = 0. \tag{21}$$

It can be proved that the director field has the minimum elastic energy of bending when $\phi$ is a harmonic function (FRANK, 1958). Director configuration around a singular point of $\phi$ is called a "disclination". A group of solutions of the Laplace equation $\Delta\phi = 0$ including disclinations is given by

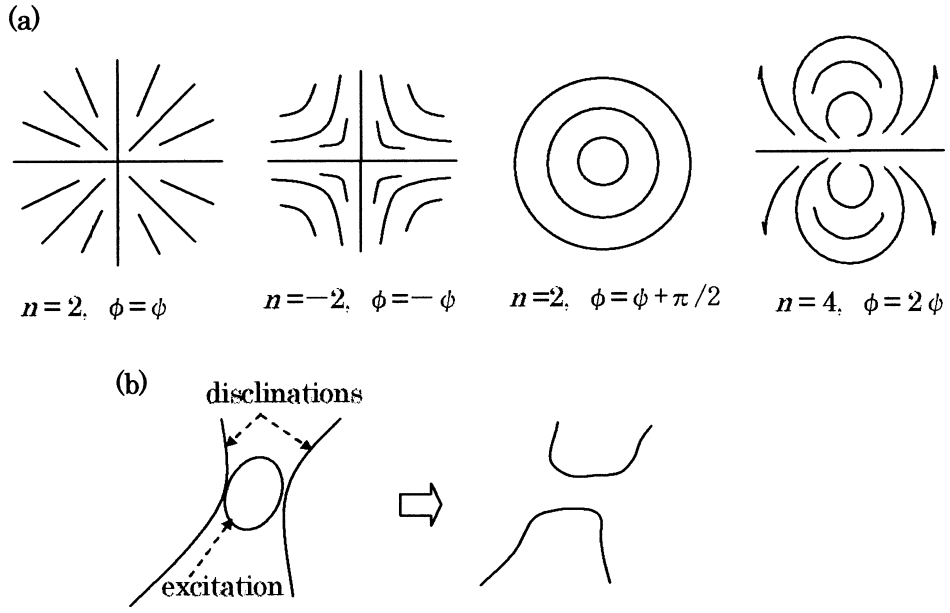


Fig. 11. (a) Some typical director fields with 2D nature. Sketches from figures in the paper of FRANK (1958), (b) a speculative sketch of reconnection process.

$$\phi = \frac{n}{2}\psi + \phi_0, \quad \psi = \tan\frac{y}{x}, \quad \phi_0 = \text{const.} \tag{22}$$

Some of the solutions are shown in Fig. 11.

Since the elastic energy of director field is concentrated in the local region around a disclination, the total energy is nearly proportional to the total length of disclination. Then, the director field will make a transition to a state with lower energy, i.e. the state with smaller disclination length, if it is attained through a reconnection of disclinations. Although existence of the reconnection process is suspected (NAGAYA *et al.*, 1992), mechanism of this process is not well understood. If an analogy with viscous fluid is allowed, superposition of a certain kind of thermal fluctuation with a ring shape, as shown in Fig. 11(b), might be one possibility for the mechanism.

## 4. Experiment and Numerical Simulation of Reconnection in Viscous Fluid

### *4.1. Experimental observation of vortex behavior*

The proposed local dynamics in the reconnection process has been confirmed through an experiment and a numerical simulation by the present author and his colaborator (KAKIZAKI, 1990; TAKAKI and KAKIZAKI, 1992). The purpose of the experiment was to measure velocity change during the reconnection process. The experimental apparatus is shown in Fig. 12.

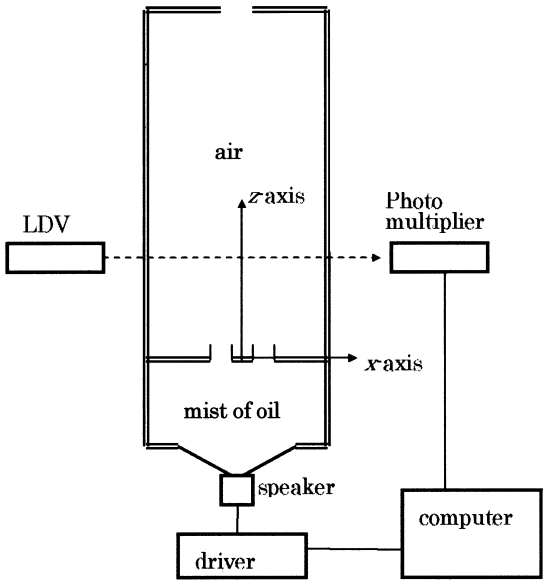


Fig. 12. Experimental apparatus.

Two vortex rings were ejected upwards side-by-side from two orifices by pushing the air by a large loud speaker. The two vortex rings made the first reconnection to produce a single elliptic vortex, which were separated through the second reconnection to two vortex rings. These motions were visualized by adding oil mist to the lower reservoir. Flow velocity was measured by the use of a laser-Doppler velocimeter.

Visualized behavior of the ejected vortices is shown in Fig. 13, which is the same as observed by OSHIMA and ASAKA (1977). In this figure the stage (a) is just after ejection, (b) in the first reconnection, (c) a new born elliptic ring and (d) in the second reconnection.

The vertical and the horizontal components of velocity on the *xz*- and *yz*-planes were measured, where the *xz*-plane contained the centers of both orifices and the *yz*-plane was set between two orifices. From these velocity components we calculated the vorticity component perpendicular to these planes. In Fig. 14 maps of velocity and vorticity components are shown for three stages of reconnection process. At the stage shown in Fig. 14(a) the fluid was circulating in the *xz*-plane, and correspondingly the vortex filaments were intersecting with the *xz*-plane, which corresponded to the stage (a) in Fig. 13. At the stage shown in Fig. 14(b) a circulating flow and a vorticity appeared in the *yz*-plane, (stage (b) in Fig. 13). Figure 14(c) shows the stage where the first reconnection was over, where a new elliptic ring intersected both with *xz*- and *yz*-planes (stage (c) in Fig. 13). This behavior of vorticity was also cinfirmed by ontaining circulations during the first reconnection, as shown in Fig. 15. In this figure, the two curves for the circulations $\Gamma_{xz}$ were obtained for the two circulating motions in the *xz*-plane, while $\Gamma_{yz}$ was from that in the *yz*-plane. We can see from this figure that the decreases of $\Gamma_{xz}$ were associated with an increase of $\Gamma_{yz}$ showing the reconnection of filaments.

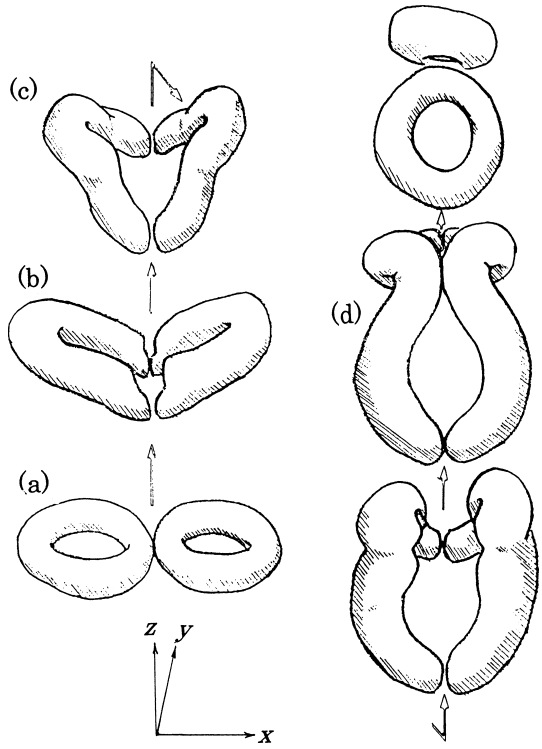


Fig. 13. Observed behavior of vortex rings from visualization pictures (from KAKIZAKI, 1990). Stages (a), (b), (c) correspond to those shown in Figs. 14, 16 and 18.

Signals of upward velocity component at two points on the center line are shown in Fig. 16. The data in Figs. 16(a) and (b) were taken at points before reconnection and during reconnection, respectively. At each point signal input was repeated number of times and 20 of them are shown here. As is seen from these figures, the signals before reconnection had a very good reproducibility, which would mean that the vortices had behaved quite regularly. On the other hand, the data during reconnection had a certain degree of fluctuation. This fluctuation suggests irregular motion of fluid during reconnection. This irregularity is considered to be consistent with the idea expressed by Eqs. (7) and (14), i.e. the reconnection proceeds by superposing a field $\boldsymbol{u}^{(r)}(t)$, which grows exponentially from an initial small value. This type of growth is common among unstable disturbances, which are influenced sensitively by background noises. In the present experiment varying flow field might have been influenced much by weak noisy background flow, leading to these fluctuating signals.

*4.2. Computation of vorticity behavior*

Numerical computation of reconnection process was made for the same boundary and initial conditions as in the experiment explained above (KAKIZAKI, 1990; TAKAKI and

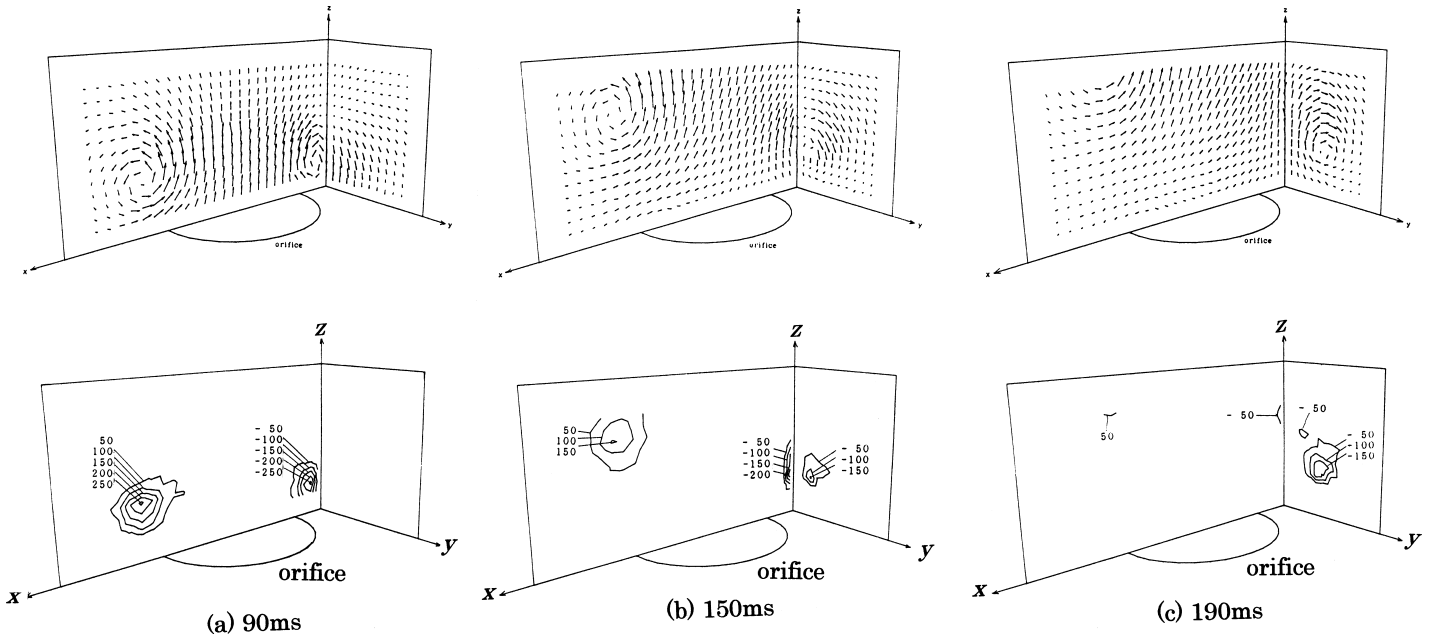


Fig. 14. Measured velocity and vorticity distributions at instants, (a) before reconnection, (b) during reconnection and (c) after the first reconnection. These three instants correspond to the three stages in Fig. 13 (from KAKIZAKI, 1990).

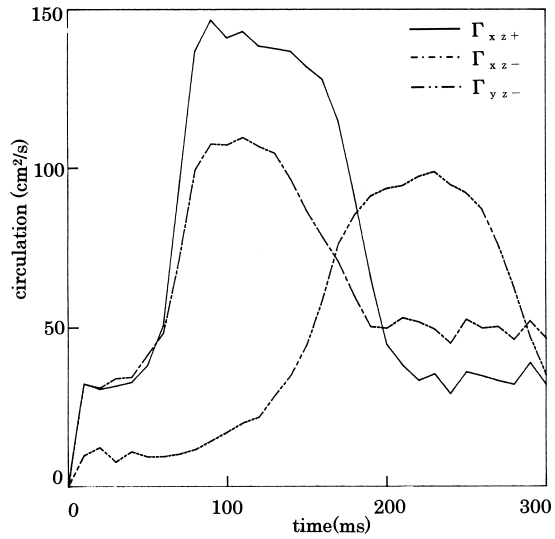


Fig. 15. Variations of circulations of vortices on *xz*- and *yz*-planes. Two vortices on the *xz*-plane were treated separately (from KAKIZAKI, 1990).

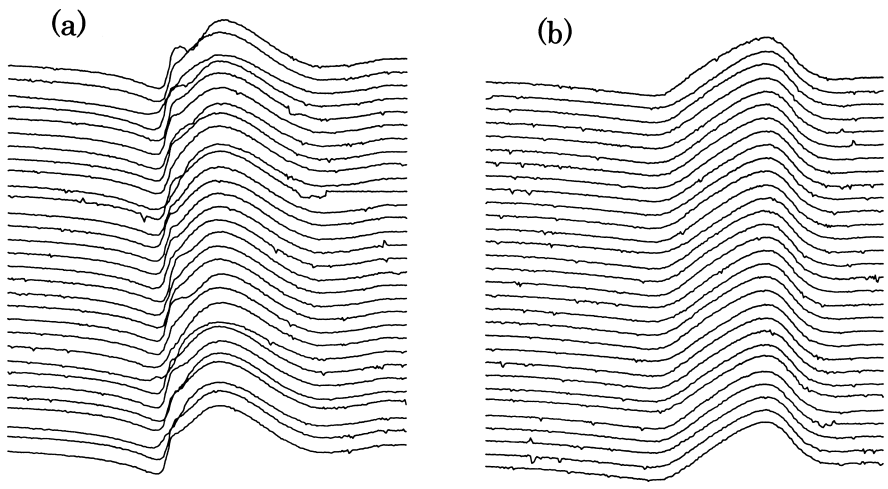


Fig. 16. Velocity signals at two points on *z*-axis, (a) before reconnection, (b) during reconnection (from KAKIZAKI, 1990).

KAKIZAKI, 1992). In the computation the difference scheme with the Crank-Nocolson method was applied. As an initial condition was that the fluid was at rest everywhere. As the boundary condition a uniform but time-dependent inlet flow (fixed after the experimental data) was assumed on the two orifice regions and zero velocity gradients was given at the

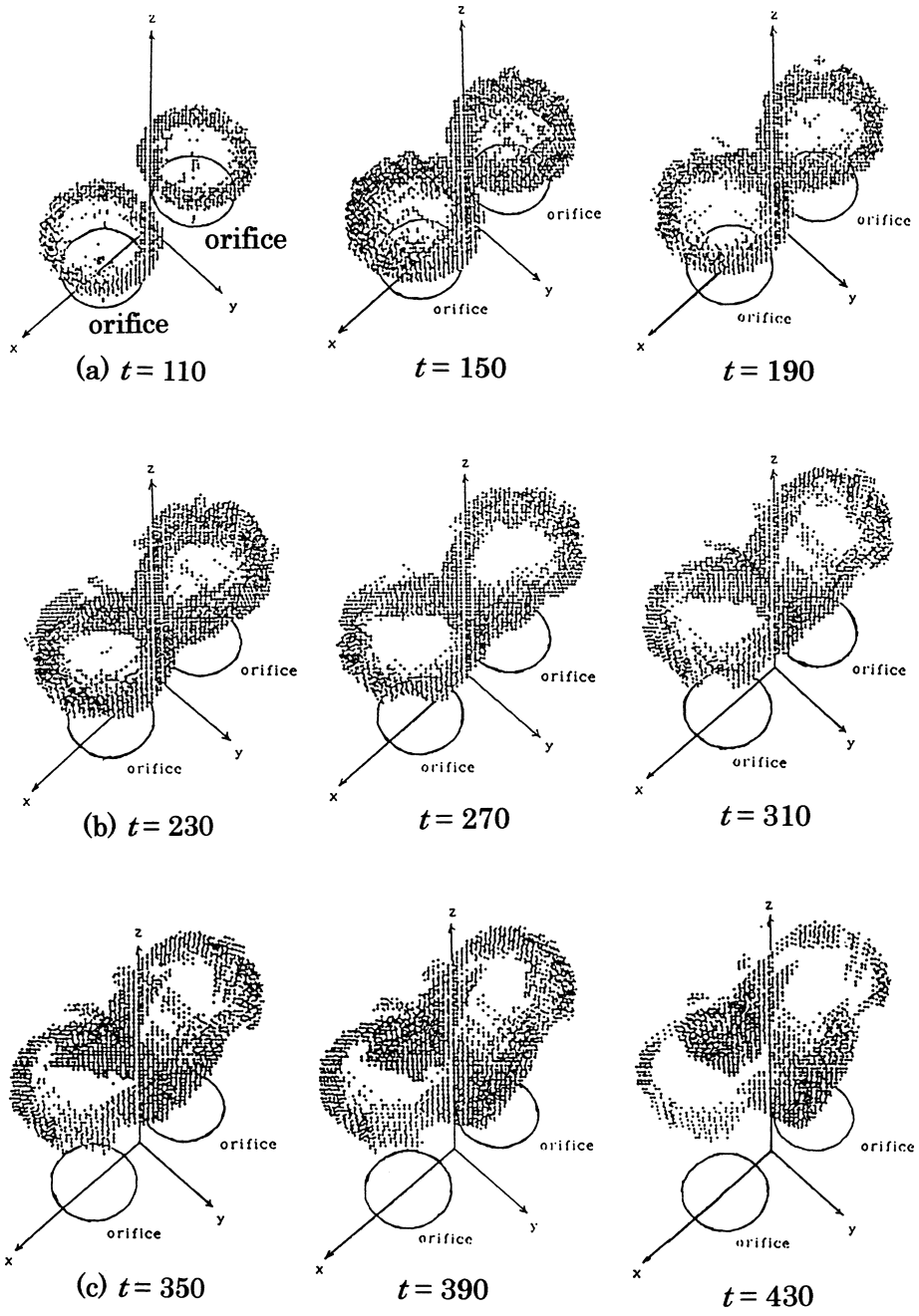


Fig. 17. Computed behavior of vortex rings, where absolute value of vorticity is shown by the dot density (from KAKIZAKI, 1990).

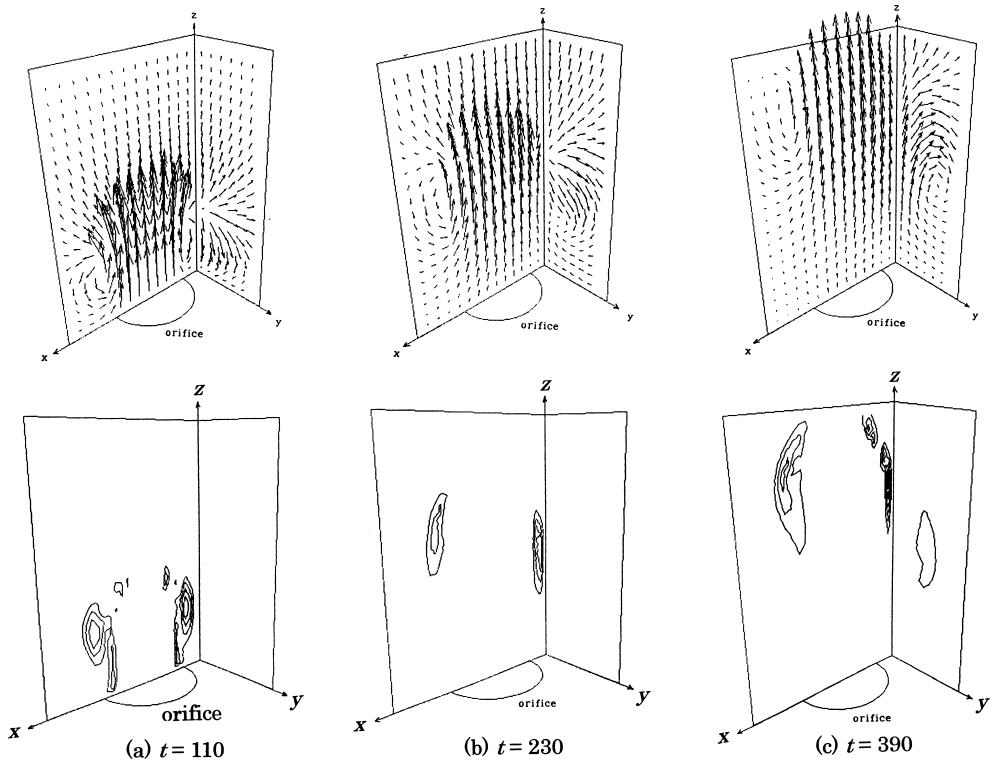


Fig. 18. Computational results for the velocity and vorticity distributions at instants, (a) before reconnection, (b) during reconnection and (c) after the first reconnection (from KAKIZAKI, 1990). These three instants correspond to the three stages in Fig. 17 and also to the experimental results shown in Fig. 14.

upper exit for a certain period. After this period zero velocity was given on all boundaries.

Figure 16 shows the computed behavior of vortex rings, where the absolute values of vorticity is shown by the dot density. This behavior confirms the visualization by the present author (Fig. 13) and that by OSHIMA and ASAKA (1977). This figure reveals more precise behavior of vorticity than the sketch (Fig. 13), i.e. weak bridges remained maintaining the original vortex filaments partly, even after reconnection. This behavior has been found by several researchers (MELANDER and HUSSAIN, 1989; KIDA *et al.*, 1991). But, in this paper this phenomenon is not discussed more, because it means an incomplete occurrence of reconnection and is out of the interest of this review.

Figures 17(a), (b) and (c) are computational results for the velocity and vorticity distributions at instants corresponding to the experimental results shown in Fig. 12. Their agreement is obvious and it confirms once more the reality of reconnection process. The difference of aspect ratios (ratios of horizontal and vertical sizes) of spaces between the experimental data and computational result is due to a restriction in the test section of the apparatus. We can see slightly faster upward movements of vortices in the computation.

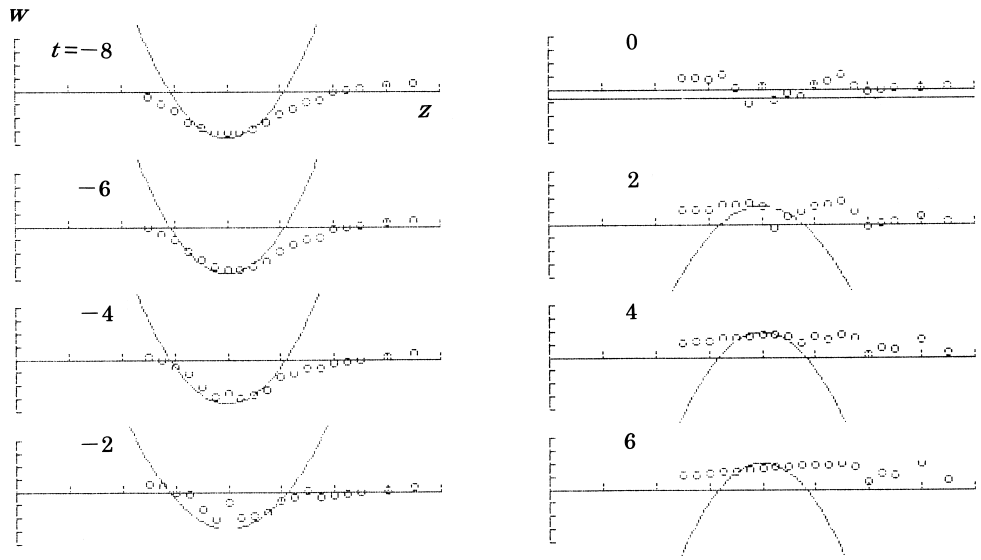


Fig. 19. Comparison of variations of $w$ (z) on the $z$-axis between theory (solid line) and experiment (circles). Values of coefficients in the theory are fixed as $w_0 = -3.5$, $\delta = -5.5$, $m = 0$, $k = -6$.

This difference is caused by the rather simplified boundary condition in the computation. The real inlet flow at the orifices was not uniform but had a velocity distribution within the orifice region, while the computation allowed a sharp cut of velocity at the orifice edge which produced a thinner vortex filament. Since thinner vortex filaments move faster, this difference of vortex behavior is well understood.

*4.3. Comparison of the experiment with the theory*

The experimental results explained above can be compared with the theory introduced in Subsec. 3.2. Since the theory is concerned with the flow in a local region where reconnection is taking place, it must be compared with the data on the $z$-axis in the apparatus (see Fig. 10). Here, the upward velocity $w(0, 0, z, t)$ in Eq. (8c) is compared with experimental data. The unknown coefficients in this solution are fixed so as to have the best matching, i.e. $w_0 = -3.5$, $\delta = -5.5$, $m = 0$ and $k = l = -6$. Note that these values are all negative while they are positive in the theory. It comes from the difference of vortex configurations between experiment and theory. The two vortex rings in the experiments produced downward velocity at the point of touching, where the reconnection took place, while in the theory the vertical velocity at the origin directs upwards initially.

By assuming these values for coefficients, we have a fairly good agreement between theory and experiment, as shown in Fig. 19. The rather flat distributions of velocity in the experiment, especially after reconnection ($t > 2$), would be due to the rather complicated behavior of vorticity in the experiment. Such a behavior is not considered in the theory. However, this agreement shows that the theory given in Subsec. 3.2 is also catching an essential feature of reconnection at least in a narrow region where it is taking place.

## 5. Discussion

In this review a general introduction to the interesting and still mysterious phenomenon called “reconnection” is given by taking examples from various physical systems. They have some common natures as listed below, which would lead to a common understanding this phenomenon although they are governed by different dynamical equations.

(i) The reconnection process is three-dimensional, transient, having a nonlinear nature and associated with dissipative effect, as is noted in Subsec. 3.2. Its dynamics will not be captured well, if any of these is lacking.

(ii) In the central region, where the reconnection is taking place, the effects of dissipation and nonlinearity (the convection effect in the case of viscous fluid) are playing equally important roles.

(iii) The convection effects are similar among different systems, while the dissipative effects depend on the nature of materials. In the case of viscous fluid and magnetic field in plasma the dissipative effects are expressed by the second derivatives of field variables associated with viscosity and conductivity. This mathematical nature makes their effects confined within a narrow region (called an inner region). On the other hand, in the cases of liquid superfluid and crystal, the dissipative effects are not well understood.

Some suggestions are given as to the future developments of researches of the reconnection process. The theory for the viscous fluid explained in Subsec. 3.2 is still far from satisfaction, because it treats only a central region of reconnection. It should be extended to the outer region or at least to the margin with it.

As for the superfluid and liquid constructing dynamics of thermal excitations with filament type seems to be a key point. Macroscopic equations available at present, such as the time-dependent Ginzburg Landau equation, would not be capable of treating the reconnection process, because it does not govern local and rapid transient states. Theories containing microscopic (or at least mesoscopic) processes explicitly are wanted, where microscopic thermal excitations may play an important role associated with certain kinds of quantum jump. A new theory might be analogous to the Langevin equation (a basic equation for the Brownian motion of small particles). Theoretical developments of the reconnection processes with drastically new ideas are expected to develop in future.

## Appendix A

The procedure to determine possible terms of expansions for velocity and vorticity components are explained here briefly.

Table 1 in Subsec. 3.2 gives the possible terms for velocity components up to the second order, which satisfy required symmetries and magnitudes of components. By adding the terms for the superposed vortex ring and vorticity (also Laplacian of the vorticity) Table 1 is extended as shown in Table A1. The vorticity components and their Laplacians can be obtained from the velocity components by applying differential operations. But, they are considered separately in the table, because only polynomials up to the second are considered. Relations between coefficients are fixed later.

Coefficients of polynomial expansions listed in Table A1 are related each other by

Table A1. Symmetries of velocity and vorticity components with respect to coordinates.

| | Initial state | | | | | | Final state | | | | | |
|---|---|---|---|---|---|---|---|---|---|---|---|---|
| | $x$ | $y$ | $z$ | 0th | 1st | 2nd | $x$ | $y$ | $z$ | 0th | 1st | 2nd |
| $u$ | odd | even | — | — | $x$ | $xz$ | odd | even | — | — | — | — |
| $v$ | even | odd | — | — | — | — | even | odd | — | — | $y$ | $yz$ |
| $w$ | even | even | — | 1 | $z$ | $x^2, z^2$ | even | even | — | 1 | $z$ | $y^2, z^2$ |
| $\omega_x$ | even | odd | — | — | — | — | even | odd | — | — | $y$ | $yz$ |
| $\omega_y$ | odd | even | — | — | $x$ | $xz$ | odd | even | — | — | — | — |
| $\omega_z$ | odd | odd | — | — | — | — | odd | odd | — | — | — | — |
| $\Delta\omega_x$ | even | odd | — | — | $y$ | | even | odd | — | — | $y$ | |
| $\Delta\omega_y$ | odd | even | — | — | $x$ | | odd | even | — | — | $x$ | |

| | Superposed vortex ring | | | | | |
|---|---|---|---|---|---|---|
| | $x$ | $y$ | $z$ | 0th | 1st | 2nd |
| $u^{(r)}$ | odd | even | even | — | $x$ | — |
| $v^{(r)}$ | even | odd | even | — | $y$ | — |
| $w^{(r)}$ | even | even | odd | — | $z - z_r$ | — |
| $\omega^{(r)}_x$ | even | odd | odd | — | — | $y(z - z_r)$ |
| $\omega^{(r)}_y$ | odd | even | odd | — | — | $x(z - z_r)$ |
| $\omega^{(r)}_z$ | odd | odd | even | — | — | — |
| $\Delta\omega^{(r)}_x$ | even | odd | odd | — | — | $y(z - z_r)$ |
| $\Delta\omega^{(r)}_y$ | odd | even | odd | — | — | $x(z - z_r)$ |

The symbol "—" means no symmetry or no term. "0th", "1st", "2nd" mean possible terms up to the second order polynomials. $z_r$ in the lower column is the average height of the two vortex rings and symmetries in $z$ direction are shown with respect to this level.

applying some relations for velocity and vorticity. They are definition of the vorticity (Eq. (2)), the continuity equation div$\boldsymbol{u}$ = 0 in each of the flow fields $\boldsymbol{u}^{(i)}$, $\boldsymbol{u}^{(f)}$, $\boldsymbol{u}^{(r)}$ and the asymptotic condition (Eq. (7)). Thus, we obtain finally the expressions given in Eqs. (8)–(10). These manipulations are rather complicated, and the precise is given in the paper by TAKAKI and HUSSAIN (1985).

## Appendix B

It is shown here that the effect of viscosity in the region between the initial vortex filaments, which leads to reconnection of those filaments.

The $x$ component of the vorticity equation (11) is applied to the $x$ component of vorticity on the $yz$-plane. This equation, then, is written as follows:

$$\left(\frac{\partial \omega_x}{\partial t}\right)_0 = -\left(u\frac{\partial \omega_x}{\partial x} + v\frac{\partial \omega_x}{\partial y} + w\frac{\partial \omega_x}{\partial z}\right)_0 + \left(\omega_x\frac{\partial u}{\partial x} + \omega_y\frac{\partial u}{\partial y} + \omega_z\frac{\partial u}{\partial z}\right) + \nu\left(\Delta\omega_x\right)_0, \qquad \text{(A1)}$$

where the suffix 0 indicates the value on the $yz$-plane.

From the assumed symmetry for the initial state (see Table A1 in Appendix A), we have $u = 0$, $v = 0$ and $\omega_x = 0$ on the $yz$-plane, hence the first and the second terms in the right-hand side of this equation vanish, and we have

$$\left(\frac{\partial \omega_x}{\partial t}\right)_0 = \nu\left(\Delta\omega_x\right)_0. \qquad \text{(A2)}$$

This equation means that a new vorticity on the $yz$-plane, which should connect two initially separated filaments, does not appear without the viscosity.

On the contrary, if we have a viscosity, the required vorticity, i.e. $\omega_x$ can appear on the $yz$-plane, which can be explained as follows. As is seen from Fig. 6(b) the values of $\omega_x$ in the region $y > 0$ is positive on both sides of $yz$-plane, and zero on it. Then, it has a minimum value on this plane and its Laplacian becomes positive. Thus, according to Eq. (A2), positive $\omega_x$ begins to grow on the $yz$-plane for $y > 0$. In the region $y < 0$, a negative $\omega_x$ appears on the $yz$-plane. Note that these signs of $\omega_x$ match to the direction of vorticity in the final state.

Once $\omega_x$ has appeared on the $yz$-plane, the first and the second terms of Eq. (A1) begins to work, and after some complicated mechanisms the final state shown in Fig. 6(d) is attained. The intermediate stage before the final state is modeled in this paper by a superposition of two vortex rings on the initial state.

## REFERENCES


ARMS, R. J. and HAMA, F. R. (1965) *Phys. Fluids*, **8**, 533.
ASKMAN, M. I. and NOBIKOV, E. A. (1988) *Fluid Dyn. Res.*, **3**, 239.
BATCHELOR, G. K. (1967) *An Introduction to Fluid Dynamics*, Cambridge Univ. Press, Chap. 7.
BETCHOV, R. (1965) *J. Fluid Mech.*, **22**, 471.
CHANDRSUDA, C., MEHTA, R. D., WEIR, A. D. and BRADSHAW, P. (1978) *J. Fluid Mech.*, **85**, 693.
CROW, S. C. (1970) *AIAA J.*, **8**, 2172.
DONNELLY, R. J. (1991) *Quantized Vortices in Helium II*, Cambridge Univ. Press.
FOHL, T. and TURNER, J. S. (1971) *Phys. Fluids*, **18**, 433.
FEYNMANN, R. P. (1955) *Progress in Low Temperature Physics*, Vol. 1, North Holland Publ. Co.
FRANK, F. C. (1958) *Disc. Faraday Soc.*, **25**, 19.
GROSS, E. P. (1961) *Nuovo Cimento*, **20**, 1766.
HAMA, F. R. (1960) *Proc. Heat Tranc. and Fluid Mech. Inst.*, **92**.
HASIMOTO, H. (1971) *J. Fluid Mech.*, **21**, 447.
HOPHINGER, E. J., BROWAND, F. K. and GAGNE, Y. (1982) *J. Fluid Mech.*, **125**, 505.
KAKIZAKI, Y. (1990) Master Thesis, Tokyo University of Agriculture and Technology.
KAMBE, T. and TAKAO, T. (1971) *J. Phys. Soc. Jpn.*, **31**, 591.

KIDA, S. and TAKAOKA, M. (1988) *Fluid Dyn. Res*., **3**, 257.
KIDA, S. and TAKAOKA, M. (1994) *Ann. Rev. Fluid Dyn*., **26**, 169.
KIDA, S., TAKAOKA, M. and HUSSAIN, A. K. M. F. (1991) *J. Fluid Mech*., **230**, 583.
MELANDER, M. V. and HUSSAIN, A. K. M. F. (1989) *Phys. Fluids*., **A1**, 633.
MELANDER, M. V. and ZABUSKY, N. J. (1988) *Fluid Dyn. Res*., **3**, 247.
NAGAYA, T., HOTTA, H., ORIHARA, H. and ISHIBASHI, Y. (1992) *Pattern Formation in Comnplex Dissipative Systems*, ed. S. Kai, World Scientific, 448 pp.
OSHIMA, Y. and ASAKA, S. (1977) *J. Phys. Soc. Jpn*., **42**, 708.
PITAEVSKII, L. P. (1961) *JETP*, **13**, 451.
SCHWARZ, K. W. (1985) *Phys. Rev*., **B31**, 5782.
SCHWARZ, K. W. (1988) *Phys. Rev*., **B38**, 2398.
TAKAKI, R. (1975) *J. Phys. Soc. Jpn*., **38**, 1530.
TAKAKI, R. (1988) Physics of vortex filaments, in *Frontiers of Physics 21*, Kyoritsu Shuppan, 1 (in Japanese).
TAKAKI, R. and HUSSAIN, A. K. M. F. (1984a) *Phys. Fluids*, **27**, 761.
TAKAKI, R. and HUSSAIN, A. K. M. F. (1984b) Turburence and chaotic phenomena in fluids, in *Proc. IUTAM Symp. 1983* (ed. T. Tatsumi), 245 pp.
TAKAKI, R. and HUSSAIN, A. K. M. F. (1985) *Proc. 5th Symp. Turb. Shear Flows*, Cornell Univ., 319 pp.
TAKAKI, R. and HUSSAIN, A. K. M. F. (1986) *Proc. 3rd Asian Cong. Fluid Mech*., 150 pp.
TAKAKI, R. and HUSSAIN, A. K. M. F. (1988) *Fluid Dyn. Res*., **3**, 251.
TAKAKI, R. and KAKIZAKI, Y. (1992) Pattern formation in complex dissipative systems, in *Proc. KIT Symp. 1991*, World Scientific, 400 pp.
TOUGH, J. T. (1982) *Progress in Low Temperature Phyics*, Vol. 8, North Holland Publ. Co.
TSUBOTA, M. and MAEKAWA, S. (1992) *J. Phys. Soc. Jpn*., **61**, 2007.
YEH, T. and AXFORD, W. I. (1970) *J. Plasma Phys*., **4**, 207.